SiliconPV 2024, 14th International Conference on Crystalline Silicon Photovoltaics
Emerging Technologies for Silicon Cells, including Tandem
https://doi.org/10.52825/siliconpv.v2i.1308

Impact of AlO_x Capping Layer Thickness for Edge Passivation of $TOPCon^2$ Shingle Solar Cell

Franck Dhainaut[1,2,*], Thibaut Desrues[1], Benoit Martel[1], Mickael Albaric[1], and Olivier Palais[2]

[1]Univ. Grenoble Alpes, CEA, Liten, Campus Ines, 73375 Le Bourget du Lac, France

[2]Aix Marseille Univ, Université de Toulon, CNRS, IM2NP, Marseille, FRANCE

*Correspondence: Author Name, franck.dhainaut@cea.fr

Abstract. This work aims at understanding the short-circuit current density losses observed on TOPCon² solar cells after AlO_x layer deposition and annealing. This approach is the one most often considered in literature for edge passivation of shingle solar cells, which suffer from heavy edge recombination losses after cutting procedures. Our solar cells feature Transparent Conductive Oxide (TCO) layers at the front and rear sides, on top of which the AlO_x edge passivation layer is deposited during Atomic Layer Deposition (ALD) process. We focus on the effect of the AlO_x layer thickness and the annealing conditions on the optical and electrical properties of the front AlO_x/TCO stack. It is found that the annealing of thick AlO_x layers induces an increase of the free carrier concentration in the TCO layer, resulting in additional parasitic absorption. A thinner AlO_x layer and/or cooler annealing conditions would limit this phenomenon, however compromising with the shingle edge passivation goal. Indeed, we see that applied to the TOPCon² shingle solar cells, less current density loss comes along with lower edge passivation level.

Keywords: Shingle Passivation, AlO_x Capping, TCO

1. Introduction

Photovoltaic technologies on the market evolve simultaneously towards high-efficiency solar cells implementing passivating contacts (TOPCon, SHJ) and cell interconnection approaches featuring small-size solar cells. One of the promising interconnection methods relies on overlapping shingle-shaped solar cells and is expected to emerge in the next few years [1]. The advantages of such a module architecture are better shading resilience [2] and reliability [3], but mostly an increased output power when compared to conventional interconnection methods [4]. This last improvement is due to an increase in the active area of the panel, which results from a metallization shading reduction (no ribbon on the front surface), the removal of in-between cell spaces, and the reduction of resistive losses allowed by a reduction of current [5]. However, high-V_{OC} (Open Circuit Voltage) solar cells performances are heavily affected by carrier recombination occurring at the edges as the perimeter-over-area ratio increases for small-size formats [6]. Moreover, the cutting of standard large solar cells into shingles created highly defective unpassivated edges. Overall, the efficiency of shingles typically drops by the order of $1\%_{abs}$ [7].

Edge passivation of silicon solar cells is therefore a subject that has recently attracted interest. The main approaches focus on edge passivation treatments after metallization, recently investigating Nafion solution sputtering [8], but mainly considering an aluminum oxide

(AlO_x) layer. The latter is formed by atomic layer deposition (ALD) and associated with a subsequent annealing step [9]-[12]. ALD is a powerful tool for depositing good-quality AlO_x layers with excellent edge conformity, as deposition takes place on all the surfaces that the gaseous chemical precursor can reach. However, this strength can also be a drawback if the layer has a negative impact on the front surface due to optical or electrical problems.

Therefore, the work presented here investigates the optical and electrical properties of AlO_x/TCO (Transparent Conductive Oxide) stacks on glass substrates. Also, we consider the feasibility of mitigating the impacts of an AlO_x layer deposition on the whole TOPCon² (double-side poly-Si/SiO_x passivated) solar cell surface by AlO_x thickness variation.

2. Experimental details

For the investigation of the optical properties of the solar cells front stack, around 70 nm of ITO:H has been sputtered on a glass substrate. As presented in **Figure 1**(a), four sample groups are then processed with either 7- or 15-nm-thick AlO_x layers and annealed either at 400°C for 3 minutes or at 350°C for 5 minutes. Optical behavior of the samples along those steps has been evaluated by spectrophotometry. Electrical properties of the TCO layer have been assessed by Hall effect.

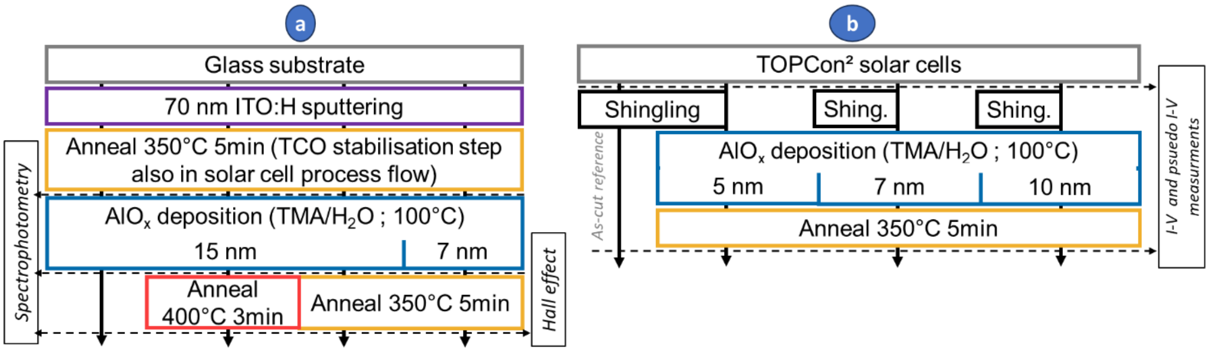

Figure 1: *Design of Experiments of (a) TCO/AlO_x optical and electrical behavior and (b) reduction of AlO_x thickness for shingle edge passivation*

For the investigation of the AlO_x thickness reduction effect when applied to shingle cells, we separated TOPCon² host cells into 4 groups with different AlO_x thicknesses, as presented in Figure 1(b). Once the cells separated into shingles, depending on their group, they underwent an AlO_x deposition of 5 to 10 nm and an annealing step at 350°C for 5 min under N_2 gas flow. For each group, some cells were kept full as references of the AlO_x deposition and annealing steps impact, independent from the edge effects. The IV and pseudo-IV parameters of the different shingle groups (measured reassembled) are compared to their respective performances before separation. Pseudo-FF is considered as an indicator of edge passivation, and short-circuit current density (J_{sc}) is monitored to evaluate the impact of AlO_x layers on the optical properties of the devices.

3. Results & discussion

Figure 2 presents the spectrophotometry measurements results. We can see that the variations induced by the AlO_x deposition, in **Figure 2**(a), appear only at short wavelengths. The parasitic absorption is also stronger for the thickest AlO_x layer. This evolution is consistent with an absorption solely from the AlO_x itself, without any modification of the TCO layer, as the AlO_x absorption coefficient is very low for the overall spectrum but increases for wavelengths < 350 nm [13].

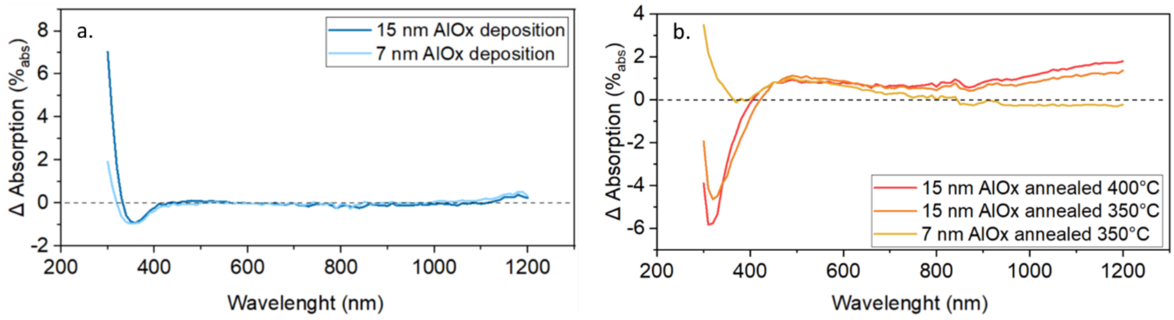

Figure 2: *Absolute evolution of the absorption following (a) AlO_x deposition (b) annealing steps (5 minutes at 350°C or 3 minutes at 400°C, under N2 gas flow)*

In Figure 2(b), we can see that the evolution of the absorption between the annealed state and the as-dep state seems influenced by both AlO_x thickness and annealing temperature. The divergent behaviors for the short wavelengths (< 400 nm) could be attributed to a difference in the evolution of AlO_x optical parameters (refraction and absorption indexes) after annealing, depending mainly on the film thickness. For longer wavelengths (> 600 nm), we notice a significant parasitic absorption for the samples with 15 nm AlO_x, which seems enhanced for high annealing temperature. This observation may lead to current density losses on the TOPCon² cell after AlO_x layer deposition and annealing. The hypothesis here would be that a modification of the TCO properties is induced by thicker AlO_x layers.

The results of Hall effect measurements of each sample group are presented in Figure 3. We see that the annealing of a 15 nm-thick AlO_x layer increases the free carrier's concentration in the TCO layer. We can also notice that the concentration levels are lower for thinner AlO_x films. This observation indicates that the excess parasitic absorption highlighted by the spectrophotometry results is in part due to free carrier absorption phenomena.

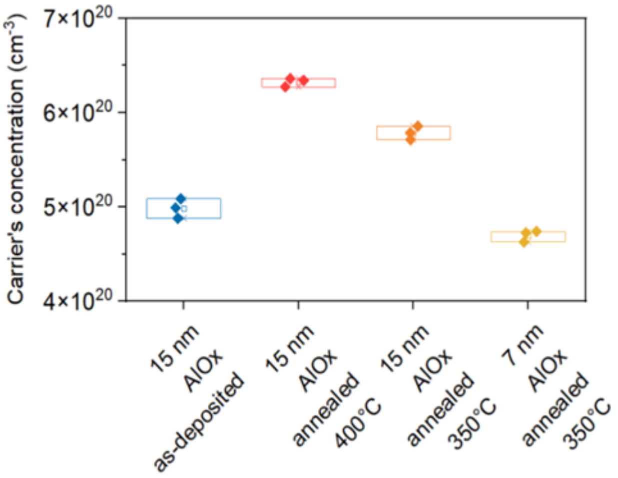

Figure 3: *Free carrier concentration in the TCO depending on the AlO_x thickness and the annealing conditions*

Notice that possible changes in the thickness of the TCO layer during the annealing step, which were not assessed here, could induce slight changes in the extracted carrier concentrations. This hypothesis should be further explored. On the other hand, it has been shown in the literature that hydrogenation of an ITO can increase its free carrier's concentration [14]. Furthermore, AlO_x layers deposited by ALD at 100°C from TMA/H_2O are hydrogen-rich [15]. Thus, this would be in agreement with the effects of both the temperature (enhanced hydrogen diffusivity) and AlO_x thickness (higher source of hydrogen) on the free carrier concentration in the ITO film.

The results at the cell level of the IV and pseudo-IV measurements are displayed in the **Error! Reference source not found.**. We confirm here the hypothesis that a reduced AlO_x thickness induces less degradation on the current density. The evolution of the p-FF can be interpreted as a lower edge passivation level with a thinner AlO_x layer. Indeed, no significant effect of the AlO_x layer is seen on the p-FF of the full cells, while we notice a lower cut-related p-FF loss for shingles with a thicker AlO_x layer on the edge. This is consistent with a better level of silicon surface passivation with increasing AlO_x layer thickness [16]. The overall efficiency losses are reduced when compared to the as-cut reference group, with an optimum compromise with a 5 nm AlO_x layer.

Table 1. *Evolution of IV and pseudo-IV parameters between host cells and processed cells. The performance of the shingle is compared with that obtained before cutting, deposition and annealing, while the performance of the whole cell is compared with that obtained before deposition and annealing.*

Group	Δ p-FF ($\%_{abs}$)	Δ J_{SC} ($mA.cm^{-2}$)	Δ η ($\%_{abs}$)
As-cut shingle ref.	-2.1	[- 0.1; 0]	-0.9
Shingle 10 nm AlO_x + anneal	-0.9	-0.4	-0.7
Shingle 7 nm AlO_x + anneal	-0.9	-0.3	-0.8
Shingle 5 nm AlO_x + anneal	-1.6	-0.2	-0.6
Full cell 10 nm AlO_x + anneal	-0.1	-0.4	-0.2
Full cell 7 nm AlOx + anneal	0	-0.3	-0.1
Full cell 5 nm AlO_x + anneal	0.1	0	0.1

4. Conclusion

By investigating the source of J_{sc} losses observed on TCO-based TOPCon² solar cells after AlO_x deposition and annealing, we found an excess parasitic light absorption from an increased free carrier concentration in the TCO layer, specifically for the 15 nm thick AlO_x layer. This phenomenon is also dependent on the post-deposition annealing temperature.

To overcome this drawback, the AlO_x layer by ALD could be localized on the edges to avoid its deposition on the front side of the cells, but that could represent an additional and potentially complex step. The reduction of the AlO_x layer thickness on the solar cells investigated here also limits these optical losses but is associated with a reduced effective edge passivation.

Data availability statement

The data that support the finding of this study are available from the corresponding author upon reasonable request.

Acknowledgment

This work was supported by the French National Research Agency (BRIGHTSIDE 22-CE05-0027 project).

Competing interests

The authors declare no competing interests.

Author contribution statement

Franck Dhainaut: Writing – review & editing, Methodology, Investigation. **Thibaut Desrues**: Supervision, Resources, Investigation, Review. **Benoit Martel**: Methodology. **Mickaël Albaric**: Supervision, Methodology, Investigation, Review. **Olivier Palais**: Supervision, Review.

References

[1] D. M. Fischer, « ITRPV PV CellTech, Berlin, March 15, 2023.
[2] N. Klasen et al., 7th Workshop on Metallization and Interconnection, Konstanz, p. 36, oct. 2017.
[3] D. Tonini et al., Energy Procedia, vol. 150, p. 36-43, sept. 2018, doi: 10.1016/j.egypro.2018.09.010.
[4] M. Mittag et al., in 2017 IEEE 44th PVSC 2017, p.1531-1536. doi: 10.1109/PVSC.2017.8366260.
[5] J. Zhao et al., IEEE Electron Device Lett., vol. 18, no 2, p. 48-50, févr. 1997, doi: 10.1109/55.553040.
[6] Fell et al., IEEE J. Photovoltaics, vol. 8, no 2, p. 428-434, mars 2018, doi: 10.1109/JPHOTOV.2017.2787020.
[7] V. Giglia, et al., in 37th European Photovoltaic Solar Energy Conference and Exhibition, online, France, sept. 2020
[8] W. Li et al., Adv Energy and Sustain Res, vol. 4, no 2, p. 2200154, févr. 2023, doi: 10.1002/aesr.202200154.
[9] P. Baliozian et al., IEEE J. Photovoltaics, vol. 10, no 2, p. 390-397, mars 2020, doi: 10.1109/JPHOTOV.2019.2959946.
[10] E. Lohmüller et al., Progress in Photovoltaics, p. pip.3680, févr. 2023, doi: 10.1002/pip.3680.
[11] B. Martel et al., Solar Energy Materials and Solar Cells, vol. 250, p. 112095, janv. 2023, doi: 10.1016/j.solmat.2022.112095.
[12] F. Dhainaut et al., EPJ Photovolt., vol. 14, p. 22, 2023, doi: 10.1051/epjpv/2023013.
[13] S. Shi et al., Advances in Condensed Matter Physics, vol. 2018, p. 1-10, 2018, doi: 10.1155/2018/7598978.
[14] M. F. Al-Kuhaili, Journal of Materials Science: Materials in Electronics, vol. 31, p. 2729–2740, 2020, doi: 10.1007/s10854-019-02813-9.
[15] G. Dingemans, Electrochemical and Solid-State Letters, 13 (3) H76-H79, 2010, doi: 10.1149/1.3276040.
[16] G. Kaur et al., IEEE J. Photovoltaics, vol. 7, no 5, p. 1224-1235, sept. 2017, doi: 10.1109/JPHOTOV.2017.2717040.